Abdominal Radiology


Published online: 15 February 2018

Abdom Radiol (2018) 43:1515–1523
https://doi.org/10.1007/s00261-018-1503-6

# Imaging findings of ovarian dysgerminoma with emphasis on multiplicity and vascular architecture: pathogenic implications

Takahiro Tsuboyama,[1] Yumiko Hori,[2] Masatoshi Hori,[1] Hiromitsu Onishi,[1] Mitsuaki Tatsumi,[1] Makoto Sakane,[1] Takashi Ota,[1] Noriyuki Tomiyama[1]

[1]Department of Radiology, Osaka University Graduate School of Medicine, 2-2, Yamadaoka, Suita, Osaka 565-0871, Japan
[2]Department of Pathology, Osaka University Graduate School of Medicine, 2-2, Yamadaoka, Suita, Osaka, Japan

## Abstract

We report the imaging findings of three ovarian dysgerminomas that coexisted with other germ cell tumors or gonadoblastomas, focusing on the distribution of tumor nests and vascular architecture, which might provide information about the pathogenesis of dysgerminomas. In a 14-year-old female with dysgerminoma and coexisting gonadoblastomas, contrast-enhanced magnetic resonance imaging (MRI) demonstrated a solid mass in the right ovary, which presented as hyperintense lobules on diffusion-weighted imaging separated by fibrovascular septa. Some small nodules were found to exist separately from the lobules (multiplicity) and to include pathological remnants of gonadoblastoma. Large tumor vessels were present at the center of the mass (central blood vessels), which were in direct contact with the ovarian veins and radiated peripherally through the fibrovascular septa. In a 35-year-old female, a mixed germ cell tumor, which was mainly composed of dysgerminoma and yolk sac tumor foci, exhibited the same vascular architecture pattern as the first dysgerminoma on contrast-enhanced computed tomography. In a 10-year-old female with a mixed germ cell tumor, contrast-enhanced MRI revealed an enlarged left ovary, which contained a large heterogeneous mass and multiple tiny nodules (multiplicity). Microscopically, the former corresponded to a yolk sac tumor, and the latter corresponded to a dysgerminoma containing remnants of gonadoblastoma. Based on these cases, the presence of tumor nest multiplicity and central blood vessels might aid the diagnosis of dysgerminoma, and these imaging findings might be indicative of the synchronous development of multiple dysgerminomas from primordial germ cells or gonadoblastomas.

*Correspondence to:* Takahiro Tsuboyama; *email:* ttsuboyama@gmail.com

**Key words:** Ovary—Dysgerminoma—Gonadoblastoma—CT—MRI

Ovarian dysgerminoma is rare, constituting 1–2% of all malignant ovarian tumors, but it is one of the most common malignant germ cell tumors [1]. Its preoperative diagnosis is important because it occurs in children and young females, and fertility-sparing surgery should be selected, regardless of the stage of the disease, which is not the case for epithelial ovarian cancer [2]. Although elevated serum levels of tumor markers, such as alpha fetoprotein (AFP), can be a clue to the diagnosis of malignant germ cell tumors, dysgerminoma is usually only associated with a high serum level of lactate dehydrogenase (LDH), which is a non-specific finding [1]. Therefore, imaging plays an important role in the diagnosis of dysgerminoma. Tanaka et al. reported that pure dysgerminoma is characterized by the detection of a lobulated solid mass divided by fibrovascular septa on computed tomography (CT) and magnetic resonance imaging (MRI) [3]. However, dysgerminomas can coexist with other germ cell tumors or gonadoblastomas [1], and to the best of our knowledge, the imaging findings of such tumors have not been reported. Therefore, we report the imaging findings of such cases, focusing on the distribution of tumor nests and vascular architecture, which might help to clarify the pathogenesis of dysgerminomas.

## Case report

### *Case 1*

A 14-year-old female was referred to our hospital due to abdominal distention. She had a regular menstrual cycle

and exhibited normal female development. Laboratory tests revealed an elevated serum LDH level (393 U/L). MRI was performed with a 3.0-T system (Discovery MR750w, GE Healthcare, Milwaukee, Wisconsin), which demonstrated a lobulated solid mass measuring 17 cm in diameter in the right ovary (Fig. 1A, B). The mass was divided into lobules and displayed intermediate signal intensity on T2-weighted imaging (T2WI) and high signal intensity on diffusion-weighted imaging (DWI) (Fig. 1A, C). Its fibrovascular septa exhibited strong enhancement on fat-suppressed contrast-enhanced T1WI (Fig. 1B). Some small nodules, which measured up to 1.5 cm and demonstrated high signal intensity on DWI, were found to exist separately from the lobules within the mass. They were considered to be separate lesions (multiplicity) (Fig. 1C). In addition, large tumor vessels were present at the center of the mass (central blood vessels), which were directly connected to the ovarian veins and radiated peripherally through the fibrovascular septa (Fig. 1A, B). Ovarian follicles represented by small cysts were seen in the contralateral ovary, but not in the affected ovary. The patient underwent right salpingo-oophorectomy and was pathologically diagnosed with stage lA dysgerminoma combined with gonadoblastomas according to the International Federation of Gynecology and Obstetrics (FIGO) classification. The resected mass was composed almost entirely of dysgerminoma, which had formed lobules intersected by fibrovascular septa, and partly of the preserved ovarian parenchyma (Fig. 1D–G). The preserved ovarian medulla contained many dilated blood vessels (Fig. 1E), which might have corresponded to the central blood vessels seen on MRI, and the preserved cortex included multiple nodular nests of dysgerminoma in association with gonadoblastomas (Fig. 1F, G), which might have corresponded to the separate small nodules seen on MRI. Only a few normal follicles were detected in the preserved cortex.

**Fig. 1.** Case 1: Dysgerminoma associated with gonadoblastoma in a 14-year-old female. **A** Two slices of coronal T2-weighted imaging showed a lobulated solid mass in the right ovary. The lobules with intermediate intensity (long arrows) were intersected by septa displaying low intensity (black arrowheads). A hemorrhagic cyst was present at the upper portion of the mass (asterisk), and the adjacent area to the cyst showed low intensity which contained multiple small nodules displaying the same intensity with the lobules (short arrows), i.e., multiplicity. Prominent flow voids were present at the center of the mass (white arrowheads), i.e., central blood vessels. **B** Two slices of coronal fat-suppressed contrast-enhanced T1-weighted imaging at the same levels with the T2-weighted imaging demonstrated central blood vessels (white arrowheads), which were connected to small vessels in the fibrovascular septa (black arrowheads). Asterisk points to the hemorrhagic cyst. **C** Axial diffusion-weighted imaging obtained at a b value of 1000 s/mm$^2$ at the level of the hemorrhagic cyst (asterisk) showed hyperintense lobules (long arrow) and multiple small nodules (short arrows). The small nodules existed separately from the lobules within the low intense area of the mass, i.e., multiplicity. **D** The cut surface of the resected mass displayed a lobulated appearance. Inset shows magnified view of a rectangular area adjacent to the hemorrhagic cyst (asterisk), which included multiple yellowish-white small nodules (circles) corresponding to the multiplicity on MRI. **E** Photomicrographs of the area adjacent to the hemorrhagic cyst (H&E, × 12.5) demonstrated preserved ovarian cortex and medulla architecture. Dilated blood vessels were observed in the medulla (arrowheads), and the diffuse infiltration of dysgerminoma cells and a normal follicle (arrow) were detected in the cortex. **F** The small nodules detected on the cut surface were demonstrated to be nodular nests of dysgerminoma (arrow) in the preserved cortex (H&E, × 12.5). **G** High-power view (H&E, × 200) showed many gonadoblastomas (arrows) within and near the nodular nests of dysgerminoma, which were composed of germ cells similar to dysgerminoma cells (white arrowheads) and sex cord-type cells (black arrowheads). These cells formed small acini containing basement membrane-type material. The other lobulated solid part of the mass was composed of typical pure dysgerminoma tissue (not shown).

## *Case 2*

A pelvic mass was noted during a health checkup in a 35-year-old unmarried female (gravida 0, para 0) with a regular menstrual cycle. She had elevated serum LDH (1554 U/L) and AFP (213 ng/mL) levels. Contrast-enhanced CT was performed with a 64-detector row CT scanner (Light Speed VCT, GE Healthcare), which demonstrated a lobulated solid mass measuring 15 cm in diameter in the left ovary (Fig. 2A). Central blood vessels were observed, and they exhibited the same vascular architecture pattern as was seen in case 1 (Fig. 2B). The right ovary had a normal appearance and contained some follicles. The patient underwent left salpingo-oophorectomy and was pathologically diagnosed with a FIGO stage lC mixed germ cell tumor, which was predominantly composed of dysgerminoma with yolk sac tumor foci.

## *Case 3*

A 10-year-old premenarchal girl presented with abdominal pain. She was found to have elevated serum LDH (363 U/L) and AFP (5616 ng/mL) levels. MRI was performed with a 1.5-T system (Ingenia, Philips Healthcare, Best, the Netherlands), which revealed a smooth outlined left ovarian mass together with dilated ovarian hilar and medullary vessels. The mass was composed of a homogeneous hyperintense area, a large heterogeneous mass measuring 8 cm in diameter, and multiple tiny nodules measuring approximately 5 mm (multiplicity) on T2WI

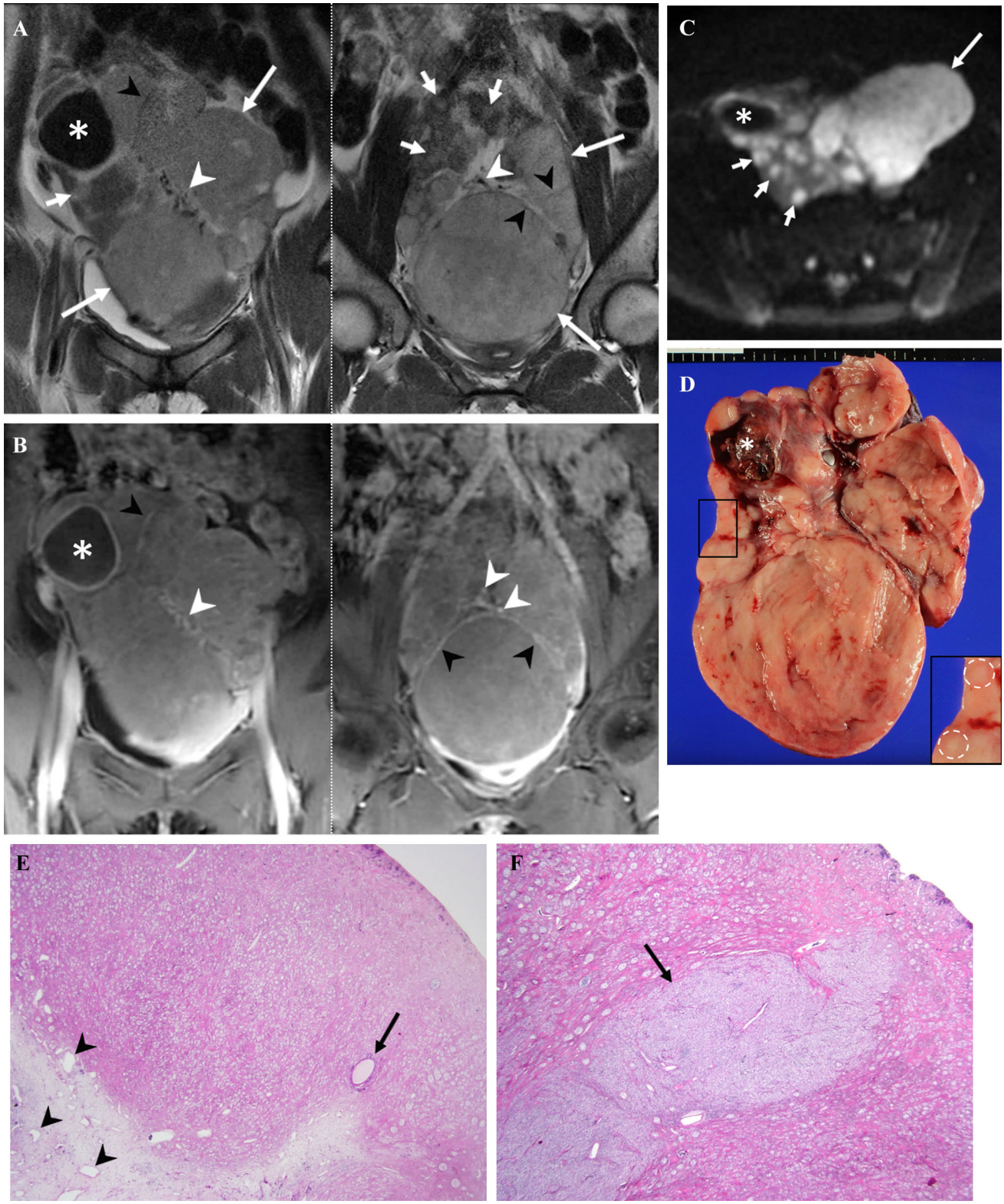


(Figs. 3A). The large heterogeneous mass displayed intermediate to high signal intensity on T2WI, high signal intensity on DWI, and strong enhancement on fat-suppressed contrast-enhanced T1WI. The multiple small nodules demonstrated intermediate signal intensity on T2WI (Fig. 3B), high signal intensity on DWI (Fig. 3C), and moderate enhancement on fat-suppressed contrast-enhanced T1WI. The right ovary had a normal appearance containing some follicles, while no follicles could be detected in the affected left ovary. The uterus appeared

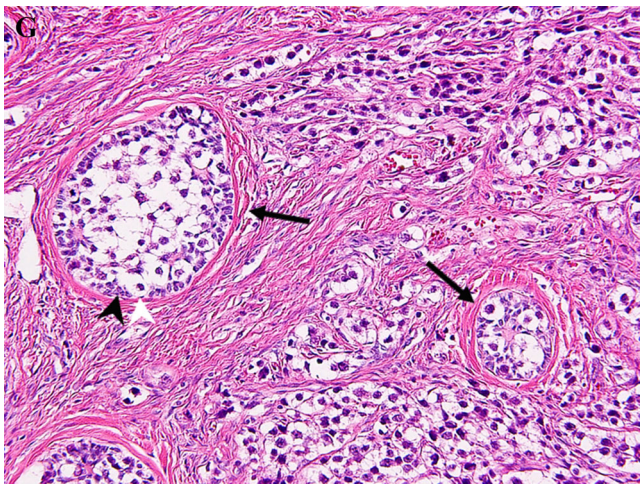


Fig. 1. continued.

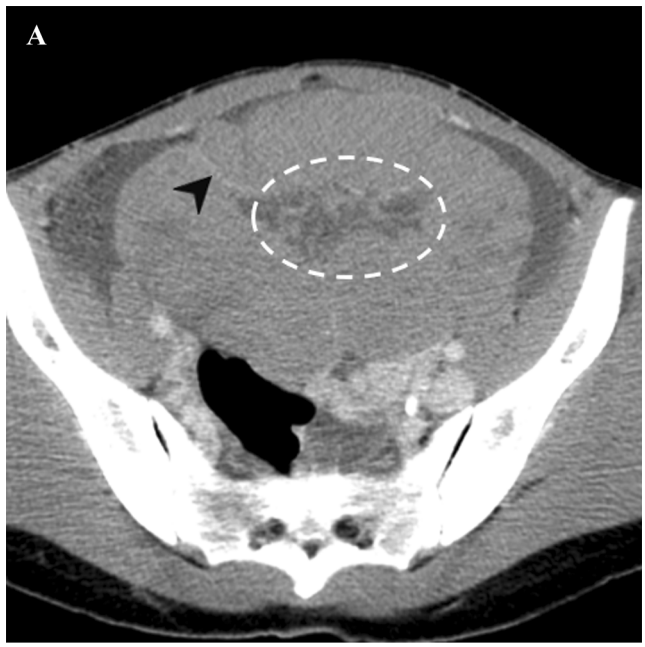


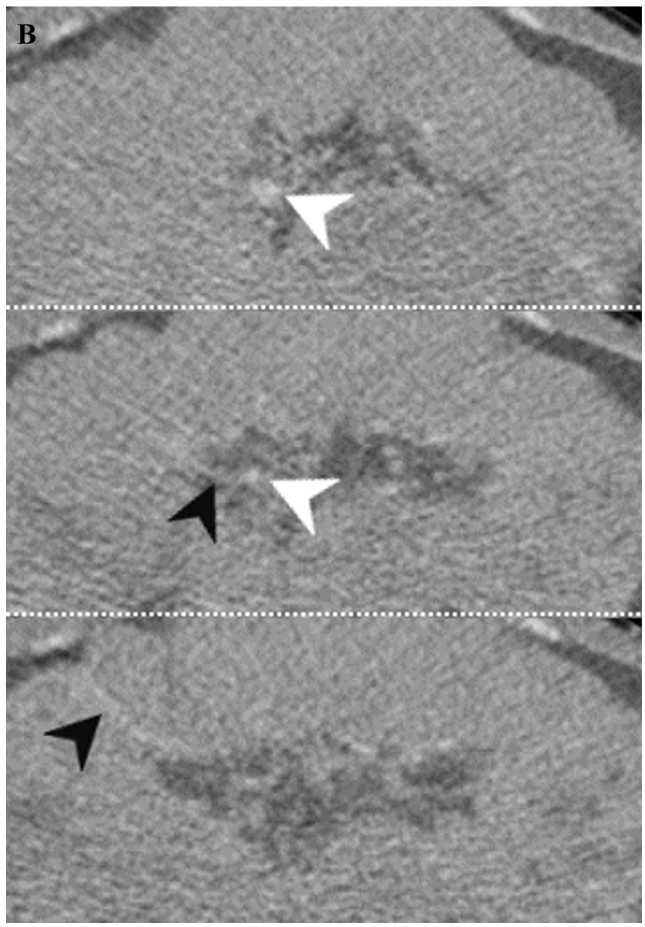


normal. The patient underwent left salpingo-oophorectomy. Microscopically, the hyperintense area, the large heterogeneous mass, and the multiple tiny nodules on T2WI were demonstrated to be an edematous ovarian parenchyma, a yolk sac tumor, and dysgerminomas with remnants of gonadoblastoma, respectively (Figs. 3D–F). Accordingly, the pathological diagnosis was a FIGO stage lC mixed germ cell tumor. Only a few follicles could be detected in the resected ovarian parenchyma. The patient did not exhibit any evidence of recurrence and reported menarche at 1 year and 4 months after surgery.

The pathology and imaging findings in the three cases were summarized in Table 1.

## Discussion

In the present three cases, the dysgerminoma components appeared as typical lobulated solid masses in cases 1 and 2, but as multiple small nodules, i.e., multiplicity, in case 3. This is probably because dysgerminoma was the predominant component in cases 1 and 2, while in case 3, the yolk sac tumor was the predominant component, and the dysgerminoma component might have arisen during the early stages of development due to the rapid growth of the coexisting yolk sac tumor. Furthermore, by paying special attention to the distribution of tumor nests, we also detected multiple small tumor nests in case 1. In cases 1 and 3, the multiplicity detected on MRI was well correlated with the small nests of dysgerminoma containing remnants of gonadoblastoma seen in the pathological examinations. Therefore, multi-

◀**Fig. 2.** *Case* 2 A mixed germ cell tumor predominantly composed of dysgerminoma with yolk sac tumor foci in a 35-year-old female. **A** Axial contrast-enhanced CT images showed a lobulated solid mass in the left ovary. Central blood vessels (circle) and small vessels in the septa (black arrowhead) were present. **B** Three consecutive slices of the contrast-enhanced CT demonstrated that the central blood vessels (white arrowheads) were connected with the small vessels within the fibrovascular septa (black arrowheads).

plicity might be indicative of the transformation of gonadoblastoma to dysgerminoma.

We encountered one more novel imaging feature of the dysgerminoma components, i.e., central blood vessels that formed via the confluence of small vessels within the fibrovascular septa at the center of the mass and were directly connected to ovarian veins. Since these vascular structure mimics that are found in normal ovaries and dilated vessels were observed in the preserved ovarian medulla during a microscopic examination in case 1 and 3, the central blood vessels might have originated from the medullary vessels of the ovary. It is worth noting that the figures for two of the three cases of pure dysgerminoma presented by Tanaka et al. seem to show central blood vessels [3]. Although the incidence of central blood vessels in dysgerminomas needs to be investigated further, no other ovarian tumor subtypes have been reported to contain central blood vessels, and thus, the presence of central blood vessels could be a useful finding for diagnosing dysgerminoma.

Based on the abovementioned imaging findings, we hypothesize that multiple synchronous dysgerminomas may develop from primordial germ cells, partially through gonadoblastomas (Fig. 4A). As each tumor nest grows, it starts to be fused with each other (Fig. 4B), and finally forms the typical lobulated solid mass (Fig. 4C). Furthermore, the medullary blood vessels of the ovary might become the central blood vessels of the tumor as the tumor grows. Therefore, dysgerminomas may appear different depending on their developmental stages. Dysgerminoma tumor nests might exhibit multiplicity during the early stages of their development (Fig. 4A) or in lesions with slow growth rates (Fig. 4B). In our case series, case 1, 2, and 3 might be at the developmental stage shown in Fig. 4B, C, and A, respectively. Since we have no clonal evidence, multiple tumor nests might arise independently (multicentric) or have a monoclonal origin (multifocal). Although the multifocal/multicentric development of dysgerminomas has never been documented in previous pathological or molecular genetic studies [4–6], we consider that imaging findings of dysgerminomas are easily explained by this concept.

Although the pathogenesis of dysgerminoma is not fully understood, two pathways have been suggested [4–6]. One involves progression from primordial germ cells via gonadoblastomas caused by the presence of Y chromosome material and resulting in gonadal dysgenesis in disorders of sex development (DSD) patients, and the other involves direct progression from primordial germ cells containing spontaneous KIT mutations in females with normal karyotypes. Hoei-Hansen et al. speculated that even in the direct pathway, some degree of gonadal dysgenesis might lead to the initiation of gonadoblastoma-like lesions [4]. Furthermore, several authors have reported that gonadoblastoma can develop in apparently normal females with 46, XX karyotypes [7–15]. Although the karyotypes of the present two patients with gonadoblastomas were not examined, they showed no clinical signs of DSD. We speculate that the incidence of

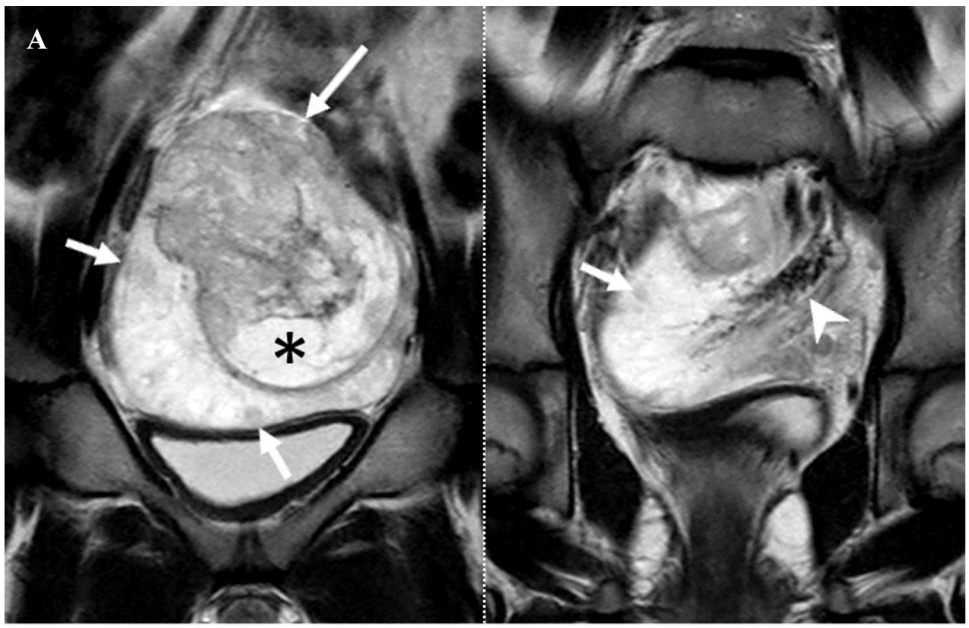
A

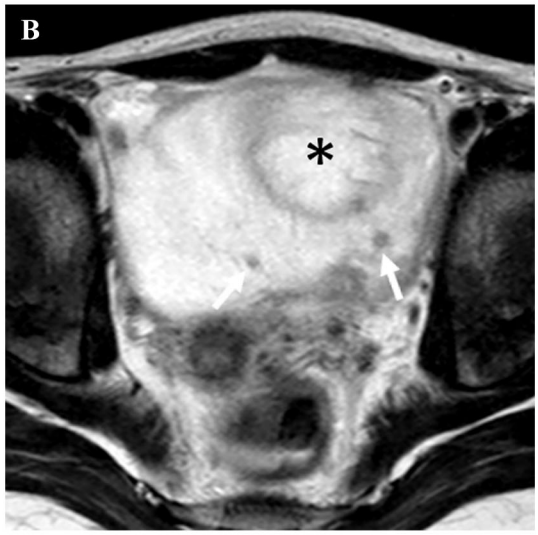
B

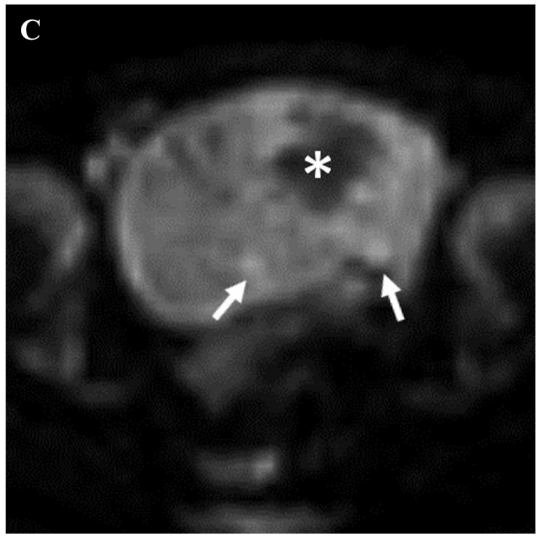
C

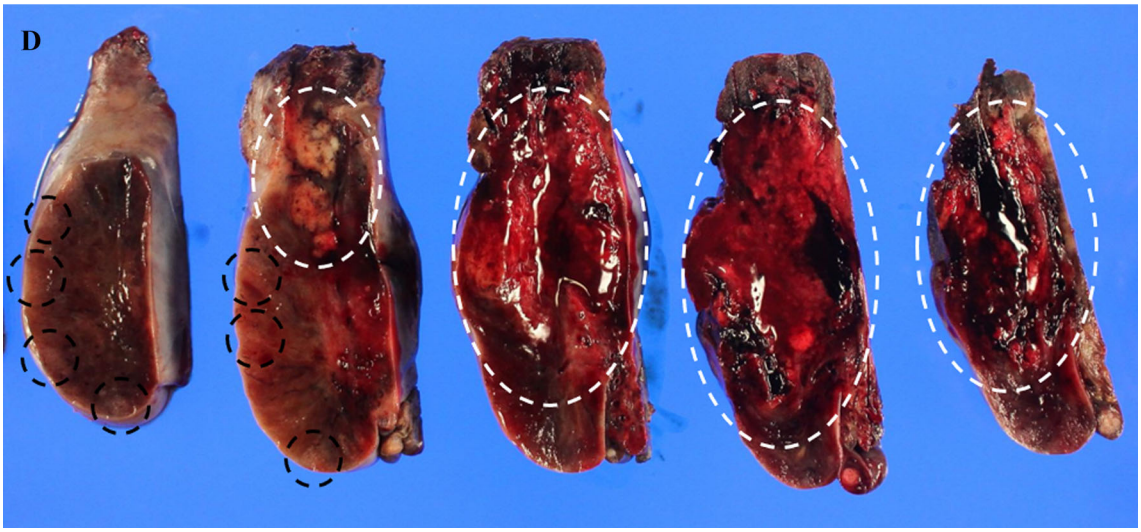
D

◀**Fig. 3.** *Case* 3 A mixed germ cell tumor composed of a yolk sac tumor and dysgerminomas associated with remnants of gonadoblastomas in a 10-year-old girl. **A** Two slices of coronal T2-weighted imaging showed a left ovarian mass with a smooth outline. The mass exhibited high signal intensity and included a large heterogeneous mass (long arrow) with necrosis (asterisk) and multiple tiny nodules (short arrows), i.e., multiplicity. Dilated medullary and hilar vessels (arrowhead) were seen. **B** Axial T2-weighted imaging showed multiple tiny nodules with intermediate intensity (arrows) within the hyperintense mass. Asterisk points to the necrosis of the large heterogeneous mass. **C** On axial diffusion-weighted imaging obtained at a b value of 1000 s/mm$^2$, the multiple tiny nodules displayed high signal intensity (arrows). The surrounding hyperintense area on T2-weighted imaging showed slight high intensity on diffusion-weighted imaging due to T2 shine-through effect. Asterisk points to the necrosis of the large heterogeneous mass. **D** Macroscopic view of the resected specimen demonstrated that the mass contained a large heterogeneous mass with hemorrhage (white circles) and multiple tiny nodules at the periphery (black circles). **E** Low-power view (H&E, × 12.5) of the multiple tiny nodules at the periphery of the mass showed that the nodules were composed of aggregation of round tumor nests (circles) within edematous ovarian parenchyma. Dilated medullary vessels (arrows) and some normal follicles (not shown) were observed. **F**. High-power view (H&E, × 200) of the circled area in Fig. 3E demonstrated that the round nests were composed of polygonal tumor cells with prominent nucleoli, which were immunoreactive for placental alkaline phosphatase, D2-40, and c-KIT (not shown). Although no sex cord stromal cells were identified, the nests contained basement membrane-type material (arrows) and were suggested to be remnants of gonadoblastomas that had been overgrown by dysgerminoma. The large heterogeneous mass was composed of a yolk sac tumor (not shown).

**Table 1.** Summary of pathology and imaging findings in three cases

| Case | Pathology | Age | Lobulated mass with septa | Multiplicity | Central blood vessels |
|---|---|---|---|---|---|
| 1 | DG + GB | 14 | + | + | + |
| 2 | DG + YST | 35 | + | – | + |
| 3 | YST + DG + GB | 10 | – | + | – |

Pathology is shown in the order of predominance
DG, dysgerminoma; GB, gonadoblastoma; YST, yolk sac tumor

gonadoblastomas in females with normal karyotypes might have been underestimated because gonadoblastomas that have been overgrown by dysgerminomas can easily be overlooked [16]. Since gonadoblastomas usually manifest as multiple tumor nests on a background of gonadal dysgenesis, it seems to be reasonable that some part of dysgerminomas undergoes multifocal/multicentric development through gonadoblastomas or gonadoblastoma-like lesions.

In conclusion, the presence of tumor nest multiplicity and central blood vessels might aid the diagnosis of dysgerminoma, and these imaging findings might be indicative of the development of multiple synchronous dysgerminomas from primordial germ cells or gonadoblastomas.

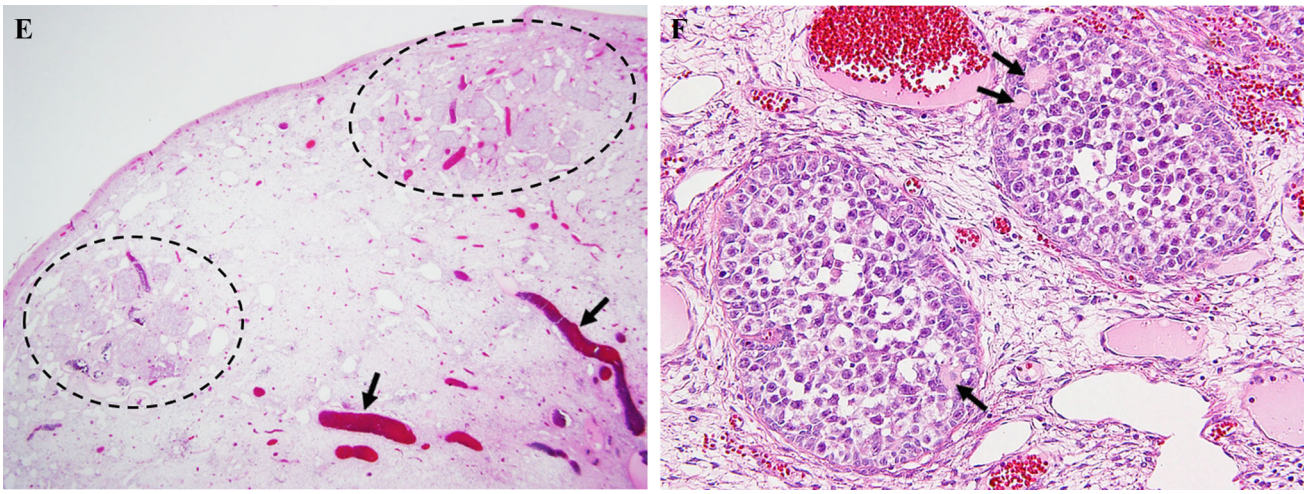


**Fig. 3.** continued.

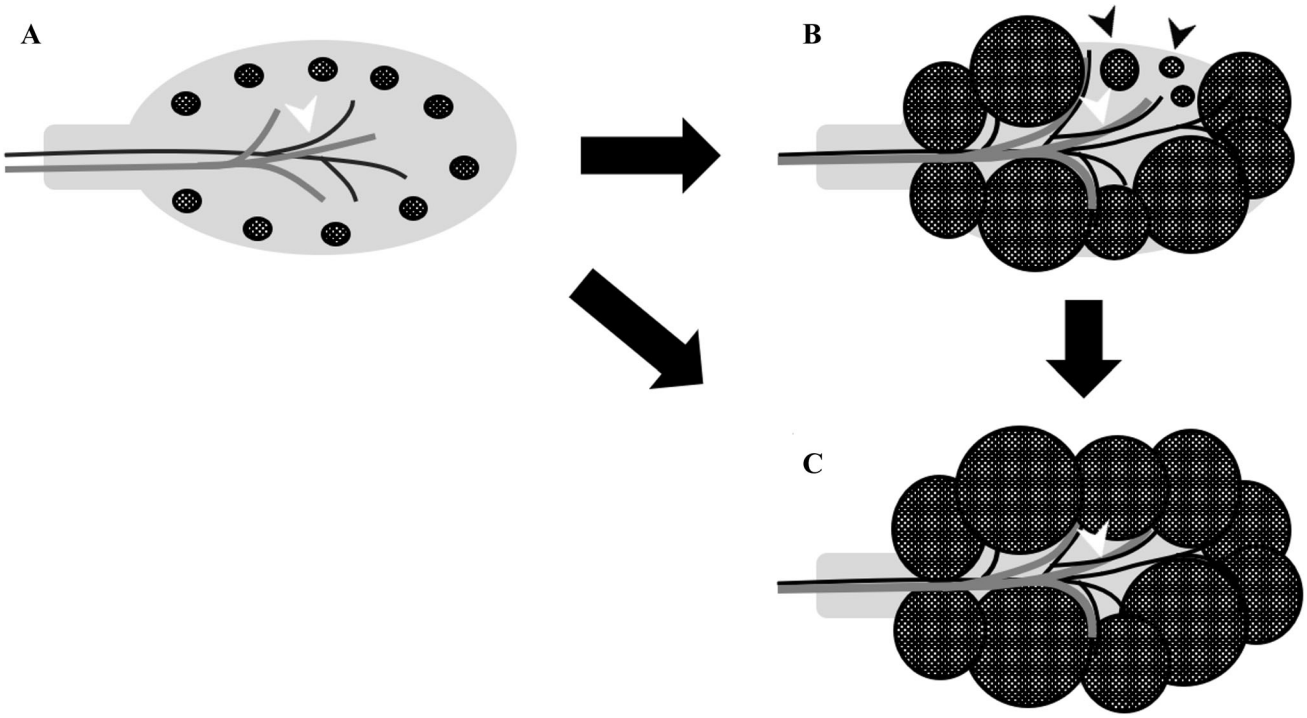


Fig. 4. Proposed pathogenesis of dysgerminoma based on the imaging findings. First, multiple synchronous dysgerminomas develop from primordial germ cells, partially through gonadoblastomas at the cortex of the ovary (**A**). Then, the tumor nests start to fuse together by their growth and to form a lobulated solid mass. In this step, small tumor nests with slow growth rates (black arrowheads) exist separately in the preserved ovarian cortex (**B**). Finally, all the tumor nests fuse together and form a lobulated solid mass (**C**). During this process, the medullary vessels of the ovary (white arrowhead) (**A**) become the central blood vessels of the tumor (white arrowhead) (**B** and **C**). Multiplicity can be observed at the early stage of development (**A**) or at the stage of incomplete fusion of the tumor nests (**B**).

**Compliance with ethical standards**

**Funding** No funding was received for this study.

**Conflict of interest** The authors declare that they have no conflict of interest.

**Ethical approval** All procedures performed in studies involving human participants were in accordance with the ethical standards of the institutional and/or national research committee and with the 1964 Helsinki declaration and its later amendments or comparable ethical standards. For this type of study formal consent is not required.

**Informed consent** Statement of informed consent was not applicable since the manuscript does not contain any patient data.

## References

1. Kurman RJ, Carcangiu ML, Herrington CS, Young RH (2014) *World Health Organization Classification of Tumours of Female Reproductive Organs*. Lyon: IARC Press
2. Gershenson DM (2007) Management of ovarian germ cell tumors. J Clin Oncol 25:2938–2943
3. Tanaka YO, Kurosaki Y, Nishida M, et al. (1994) Ovarian dysgerminoma: MR and CT appearance. J Comput Assist Tomogr 18:443–448
4. Hoei-Hansen CE, Kraggerud SM, Abeler VM, et al. (2007) Ovarian dysgerminomas are characterised by frequent KIT mutations and abundant expression of pluripotency markers. Mol Cancer 6:12
5. Pauls K, Franke FE, Büttner R, Zhou H (2005) Gonadoblastoma: evidence for a stepwise progression to dysgerminoma in a dysgenetic ovary. Virchows Arch 447:603–609
6. Hersmus R, Stoop H, van de Geijn GJ, et al. (2012) Prevalence of c-KIT mutations in gonadoblastoma and dysgerminomas of patients with disorders of sex development (DSD) and ovarian dysgerminomas. PLoS ONE 7:e43952
7. McCuaig JM, Noor A, Rosen B, et al. (2017) Case report: Use of tumor and germline Y chromosomal analysis to guide surgical management in a 46, XX female presenting with gonadoblastoma with dysgerminoma. Int J Gynecol Pathol 36:466–470
8. Kanagal DV, Prasad K, Rajesh A, et al. (2013) Ovarian gonadoblastoma with dysgerminoma in a young girl with 46, XX karyotype: a case report. J Clin Diagn Res 7:2021–2022
9. Esin S, Baser E, Kucukozkan T, et al. (2012) Ovarian gonadoblastoma with dysgerminoma in a 15-year-old girl with 46, XX karyotype: case report and review of the literature. Arch Gynecol Obstet 285:447–451
10. Koo YJ, Chun YK, Kwon YS, et al. (2011) Ovarian gonadoblastoma with dysgerminoma in a woman with 46XX karyotype. Pathol Int 61:171–173
11. Yilmaz B, Gungor T, Bayramoglu H, Soysal S, Mollamahmutoglu L (2010) Bilateral ovarian gonadoblastoma with coexisting dysgerminoma in a girl with 46, XX karyotype. J Obstet Gynaecol Res 36:697–700

12. Cooper C, Cooper M, Carter J, et al. (2007) Gonadoblastoma progressing to dysgerminoma in a 55-year-old woman with normal karyotype. Pathology 39:284–285
13. Erdemoglu E, Ozen S (2007) Ovarian gonodoblastoma with yolk sac tumor in a young 46, XX female: case report. Eur J Gynaecol Oncol 28:516–518
14. Zhao S, Kato N, Endoh Y, et al. (2000) Ovarian gonadoblastoma with mixed germ cell tumor in a woman with 46, XX karyotype and successful pregnancies. Pathol Int 50:332–335
15. Obata NH, Nakashima N, Kawai M, et al. (1995) Gonadoblastoma with dysgerminoma in one ovary and gonadoblastoma with dysgerminoma and yolk sac tumor in the contralateral ovary in a girl with 46, XX karyotype. Gynecol Oncol 58:124–128
16. Scully RE (1970) Gonadoblastoma. A review of 74 cases. Cancer 25:1340–1356